Hydrothermal synthesis of novel Mn_3O_4 nano-octahedrons with enhanced supercapacitors performances†

Hao Jiang,[ab] Ting Zhao,[b] Chaoyi Yan,[b] Jan Ma*[ab] and Chunzhong Li[c]

Received 14th April 2010, Accepted 17th June 2010
DOI: 10.1039/c0nr00257g

Uniform and single-crystalline Mn_3O_4 nano-octahedrons have been successfully synthesized by a simple ethylenediaminetetraacetic acid disodium salt (EDTA-2Na) assisted hydrothermal route. The octahedron structures exhibit a high geometric symmetry with smooth surfaces and the mean side length of square base of octahedrons is ~160 nm. The structure is reckoned to provide superior functional properties and the nano-size achieved in the present work is noted to further facilitate the material property enhancement. The formation process was proposed to begin with a "dissolution–recrystallization" which is followed by an "Ostwald ripening" mechanism. The Mn_3O_4 nano-octahedrons exhibited an enhanced specific capacitance of 322 F g^{-1} compared with the truncated octahedrons with specific capacitances of 244 F g^{-1}, making them a promising electrode material for supercapacitors.

1. Introduction

The past few years have witnessed an increasing trend towards synthetic fabrication of nanostructured materials owing to their unusual mechanical, electrical and optical properties.[1–4] Nevertheless, control over nanostructure morphologies is still noted to be one of the most essential challenges for the fundamental understanding and practical applications of nanoscale induced properties.[3,5] In the twenty-first century, energy storage has emerged to be one of the major topics, alongside the development of alternative energy sources. Nanostructured materials are found to be promising for electrochemical energy storage applications and have led to the development of new energy storage devices.[4,6,7] Among them, supercapacitors, also known as electrochemical capacitors or ultracapacitors, have attracted much attention because they can instantaneously provide a higher power density than batteries and a higher energy density than conventional dielectric capacitors, which makes them probably the most important next generation energy storage device.[8–10] For the electrode materials of supercapacitors, manganese oxides, particularly Mn_3O_4 where nanostructure could play an essential role, have been considered as one of the most attractive materials due to their low cost, great environmental compatibility and good specific capacitance.[11–16]

It has been noted that the behavior of nanomaterials strongly depends on the size, shape, dimensionality and morphology of their internal structures.[17–19] Recently, the synthesis of octahedrons composed of eight {111} crystal planes, which led to some exciting properties, have been the focus of intensive research.[20–22] For example, Cho *et al.*[20] have reported Au nano-octahedrons with well-defined shape by a modified polyol process in PEG 600 solution, which exhibited attractive optical properties. Zhou *et al.*,[21] on the other hand, have developed a biomolecule-assisted hydrothermal route to the fabrication of magnetite (Fe_3O_4) micro-octahedrons showing a discharge capacity of *ca.* 600 mA g^{-1} in the first cycle and a discharge voltage of 0.92 and 0.74 V, respectively. Most recently, Lv *et al.*[23] synthesized Mn_3O_4 micro-octahedrons by hydrothermal treatment of $KMnO_4$ in the dodecylamine–Na_2SO_3–ethanol/dedecylamine–ethanol system with arris range of 1–3 μm, which indicated excellent sensing characteristics for acetone. However, they paid little attention to the electrochemical properties due to the material's large micro-size and low BET surface area. It is, nevertheless, noted that Xie *et al.*[24] and Liu *et al.*[15] have reported the advantage of nano-structure *via* their synthesis of spinel Mn_3O_4 layered nano-architectures and Mn_3O_4 nanoparticles loaded on multi-walled carbon nanotubes, where improved capacitive performances were observed.

The above reports have inspired the present work, where a simple route was developed to synthesize uniform and single-crystalline Mn_3O_4 nano-octahedrons, firstly by an EDTA-2Na assisted hydrothermal route. The mean side length of the square base of octahedrons is ~160 nm. The electrochemical behavior of the as-obtained Mn_3O_4 nano-octahedrons was examined by cyclic voltammetry, and the results indicated that the specific capacitance could reach 322 F g^{-1}, which would be a promising electrode material for supercapacitors.

2. Experimental procedures

All the reagents used in the experiments were analytical grade (purchased from Sigma-Aldrich) and used without further purification. In a typical synthesis, 2 ml of 0.5 M EDTA-2Na and 5 ml of 0.2 M potassium permanganate ($KMnO_4$) aqueous solution were mixed together and put into a 50 ml Teflon cup, then filled with distilled water up to 70% of the total volume. The pH value of the solution was adjusted to ~6.0 using 2 M HNO_3

[a]*Temasek Laboratories, Nanyang Technological University, Singapore, 637553, Singapore. E-mail: asjma@ntu.edu.sg*
[b]*School of Materials Sience and Engineering, Nanyang Technological University, Singapore, 639798, Singapore*
[c]*Key Laboratory for Ultrafine Materials of Ministry of Education, School of Materials Science and Engineering, East China University of Science & Technology, Shanghai, 200237, People's Republic of China*
† Electronic supplementary information (ESI) available: TEM images; EDTA-2Na reaction details. See DOI: 10.1039/c0nr00257g

aqueous solution under vigorous magnetic stirring. The Teflon-lined autoclave was sealed tightly and maintained at 180 °C for 4 h and then naturally cooled down to room temperature. The precipitates were collected by filtration, washed several times with distilled water and absolute ethanol, and finally dried at 60 °C for 6 h.

The as-prepared products were characterized with X-ray powder diffractometer (XRD; Shimadzu XRD-6000, Cu-Kα radiation) at a scan rate of 2 °C min^{-1}, scanning electron microscopy (FESEM; JEOL, JSM-7600F) and transmission electron microscopy (TEM; JEOL, JEM-2100F) equipped with an X-ray energy-dispersive spectrometer (EDS). The investigations of the as-obtained products, electrochemical performances (Autolab PGSTAT30 potentiostat) were conducted using a three-electrode mode in a 1 M Na_2SO_4 solution. The working electrodes were prepared by mixing Mn_3O_4 powder (80 wt%) as active material with acetylene black (15 wt%), and poly(tetrafluoroethylene) (5 wt%). A small amount of *N*-methylpyrrolidinone was then added to the mixture. The mixture was dropped onto graphite paper and dried at 80 °C overnight to removal the solvent. The reference electrode and counter electrode were Ag/AgCl electrode and platinum, respectively. Standard CV curves were measured between −0.05 and 0.95 V.

3. Results and discussion

The field-emission scanning electron microscopy (FESEM) images in Fig. 1(A–C) show the general morphology of the Mn_3O_4 nano-octahedrons synthesized in this work. These octahedrons consist of two inverted pyramids attached at their square base and are bounded by eight triangular facets. The edges between the facets are sharp and surface of all the facets were very smooth with no obvious defects (Fig. 1C). The mean side length of square base of octahedrons was ~160 nm. The phase of the products was characterized by X-ray diffractometry, and the pattern was shown in Fig. 1D. The strong and sharp diffraction peaks in the XRD pattern indicate that the as-obtained products are well crystallized. The products are composed of two phases of manganese oxides, which are the hausmannite Mn_3O_4 (JCPDS 24-0743) for the mainly part and a very small fraction peaks marked with asterisks (*) at 2θ value of 28.8° and 37.5° assigned to the pyrolusite MnO_2 (JCPDS 24-0735). No characteristic peaks from other impurities are detected.

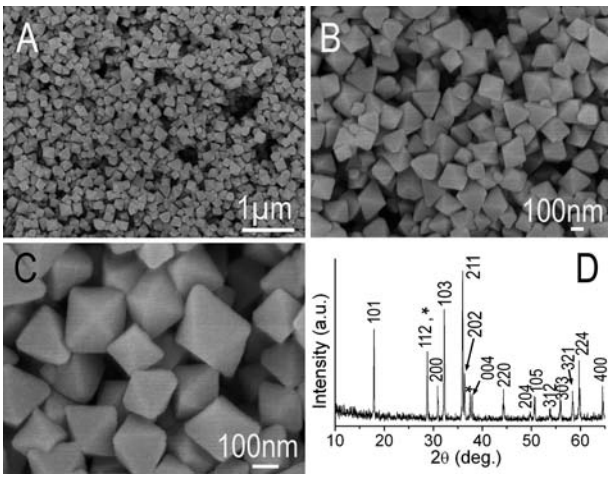

Fig. 1 (A–C) different magnification SEM image of the Mn_3O_4 nano-octahedrons, (D) the corresponding XRD pattern.

TEM image of the Mn_3O_4 nano-octahedrons (Fig. 2A) shows the product has a uniform tetragonal projected shape, consistent with the octahedron morphologies observed by FESEM. Fig. 2B gives a typical high-magnification TEM image of an individual nano-octahedron, and the corresponding edge outlines are depicted in Fig. 2C, which exhibit a high geometric symmetry of the examined octahedron with smooth surfaces. An analysis by energy-dispersive X-ray spectroscopy (EDS), Fig. 2D, confirms that the crystals are made of Mn and O with a chemical formula of $Mn_3O_{4.3}$, including 85% Mn_3O_4 and 15% MnO_2, which is in agreement with the mixed Mn_3O_4-MnO_2 manganese oxide system verified by the XRD pattern of Fig. 1D. Fig. 2(F,G) show the HRTEM images of two typical vertexes of the octahedron. The well-resolved lattice fringes give an interplanar spacing of 0.25 nm and 0.27 nm, which are in good agreement with the distance of the (211) and (103) planes, respectively. The corresponding SAED pattern (Fig. 2H) of an individual Mn_3O_4 nano-octahedron (Fig. 2E) shows the single-crystalline nature.

It is noted that the crystallographic morphology of Mn_3O_4 can be influenced by many experimental parameters, such as pH value of the reaction solution, precursor and temperature. In the present work, the pH value plays an important role for the formation of uniform Mn_3O_4 nano-octahedrons. Without the addition of HNO_3, some unordered nanostructures can only be obtained (ESI, Fig. S1†). When the pH value was decreased to below 3.0, no products are observed. Furthermore, to understand the growth mechanism of the uniform Mn_3O_4 nano-octahedrons, detailed time-dependent shape evolution studies were also carried out. As shown in Fig. 3A, the products collected at 1.5 h consisted of nanorods with diameters of ~40 nm. When the reaction time was increased to 2 h, some nano-octahedrons with good geometric symmetry began to appear (Fig. 3B). As the reaction proceeded for 3 h, the nanorods disappeared and all of

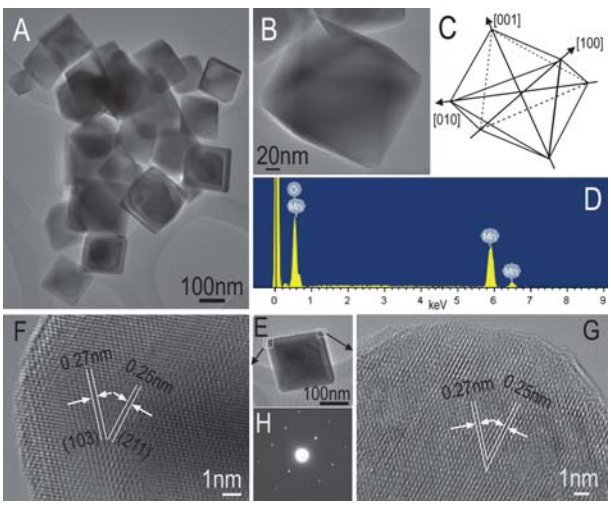

Fig. 2 (A–D) TEM image and EDS spectrum of the as-obtained Mn_3O_4 nano-octahedrons. (B) A typical high-magnification TEM image of an individual nano-octahedron with smooth surfaces; the corresponding edge outlines are depicted in (C). (F,G) HRTEM images taken from the white box areas from (E), respectively, and (H) ED pattern.

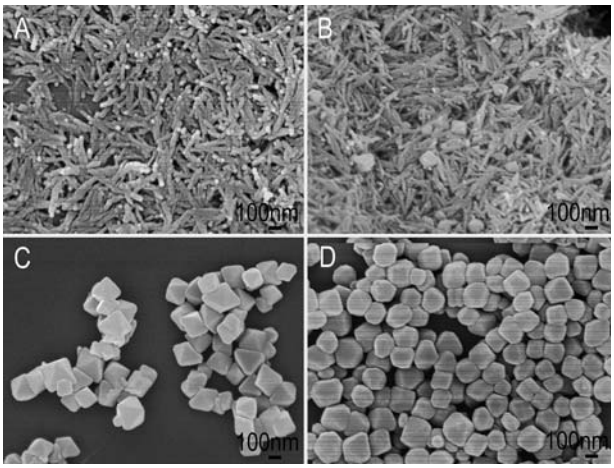

Fig. 3 (A–D) FESEM images of the Mn_3O_4 nano-octahedrons for different reaction times: (A) 1.5 h; (B) 2 h; (C) 3 h; (D) 8 h.

the products were nano-octahedrons (Fig. 3C). After 4 h of the hydrothermal treatment, well-defined regular octahedrons were obtained (Fig. 1). However, upon further increase of the reaction time to 8 h, the shape of the products transformed from octahedrons to truncated octahedrons (Fig. 3D).

Based on the time-dependent morphology evolution described above, the formation process of Mn_3O_4 nano-octahedrons could be proposed to begin with "dissolution–recrystallization" as the first step, followed by "Ostwald ripening" mechanism as the second step. At the initial stage, a large amount of nanocrystallites nucleate and grow into nanorods to minimize the overall energy of the system. However, the nanorods are just intermediate products and are not stable. After reaction for 2 h, some of the nanorods dissolve with the emergence of nano-octahedrons. When the reaction proceeds to 3 h, all of the nanorods have transformed into nano-octahedrons. This suggests that the dissolution of nanorods and the growth of nano-octahedrons occur simultaneously during the hydrothermal treatment process. Further increase of the reaction time results in the development of larger well-defined and uniform nano-octahedrons, and finally grow into truncated octahedrons based on the Ostwald ripening process.[25,26] As reported by Wang,[27] the ratio (R) of the growth rate along the <100> to <111> directions determines the geometrical shape of a crystal. The octahedron consisting of eight highly stable {111} planes resulted from a much higher growth rate along the <100> direction than along the <111> direction due to the lowest energy of the {111} surfaces. In addition, it should be noted that EDTA-2Na is a strong coordinating agent, which could form a very stable complex by coordinating with MnO^- and modify the growth rate of the Mn_3O_4 crystal by binding crystal facets.[28–30] The chemical reactions are described in detail in the ESI.† As a result, the growth on the directions were retarded and thus led to anisotropic growth.[31,32] This was confirmed by the fact that the solution color changed from purple to black–brown soon after the addition of EDTA-2Na. The complex provides the octahedrons a chemical environments for the formation of Mn_3O_4 nano-octahedrons.[33] Moreover, the suitable pH value favors the faster growth along <100> compared to that along <111>, and results in the formation of uniform Mn_3O_4 nano-octahedrons.

Cyclic voltammetry (CV) was employed to characterize the capacitive performances of the Mn_3O_4 nano-octahedrons, as shown in Fig. 4(A,B). The CV curves were recorded with the samples first stabilized by 200 CV cycles. It can be clearly observed that both of the CV curves show rectangular shape and do not significantly change with the increasing scan rates, indicating that the Faraday redox reactions are electrochemically reversible.[34,35] At the scan rates of 5, 20, 50 and 100 mV s^{-1}, the corresponding specific capacitances of Mn_3O_4 nano-octahedrons were 322, 288, 244 and 195 F g^{-1}, respectively. These results demonstrate that Mn_3O_4 nano-octahedron is a better candidate for an electrochemical capacitor electrode compared with spinel Mn_3O_4 layered nanoarchitectures[24] (133 F g^{-1} at scan rate of 50 mV s^{-1} with potential window of 0.9 V), Mn_3O_4 hexagonal nanoplates[36] (237 F g^{-1} with potential window of 0.8 V) and Mn_3O_4 nanoparticles[36] (226 F g^{-1}), and Mn_3O_4 thin films[37] (284 F g^{-1} and 0.12 F cm^{-1}). Furthermore, Liu *et al.*[15] reported the synthesis of Mn_3O_4 nanoparticles loaded on multi-walled carbon nanotubes with a high specific capacitance of 420 F g^{-1} at scan rate of 5 mV s^{-1}. However, in this case the potential window was only 0.7 V. The enhancement in the capacitance of Mn_3O_4 nano-octahedron may be ascribed to the exposed {111} surfaces,[21] which may be beneficial to intercalation/deintercalation of Na^+ and electrons. To endorse this point, the CV curves of Mn_3O_4 truncated nano-octahedrons were also

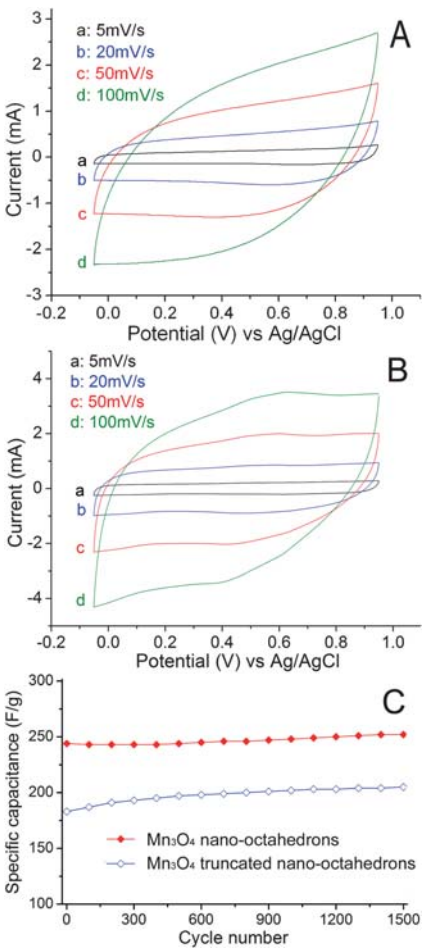

Fig. 4 CV curves of the Mn_3O_4 nano-octahedrons (A) and trancated nano-octahedrons (B) at different scan rates; (C) cycle life data at 50 mV s^{-1}.

investigated, as shown in Fig. 4B. At the scan rates of 5, 20, 50, 100 mV s^{-1}, the corresponding specific capacitances were 244, 237, 205, 170 F g^{-1}, respectively. This result further implies that the electrochemical properties of Mn_3O_4 are related to their exposed crystal facets, *i.e.* preferring the {111} surfaces. The electrochemical stabilities were investigated by repeating the CV test at a scan rate of 50 mV s^{-1} for 1500 cycles, and the good cycling stability results were shown in Fig. 4C. It can be noted that the specific capacitance increased slightly (from the initial 244 F g^{-1} to 252 F g^{-1} after 1500 cycles for the Mn_3O_4 nano-octahedrons). The increase of specific capacitance values may be due to the activation effect of electrochemical cycling.[24] Similar phenomena were also observed by Xie *et al.*[24] and Li *et al.*[38] when they investigated the electrochemical stability of spinel Mn_3O_4 layered structures and MnO_2 multilayer nanosheet clusters, respectively. Detailed studies need to be done in the near future for optimizing the use of this electrode in supercapacitors.

4. Conclusions

In summary, uniform and single-crystalline Mn_3O_4 nano-octahedrons have been successfully synthesized by a simple EDTA-2Na assisted hydrothermal route. The mean side length of square base of octahedrons is ~160 nm with smooth surfaces. The formation process was proposed to begin with the first step dissolution of nanorods accompanied with recrystallization of nano-octahedrons, followed by the second step on the formation of uniform nano-octahedrons and truncated nano-octahedrons by Ostwald ripening mechanism. The CV studies show that the Mn_3O_4 nano-octahedrons exhibit an enhanced specific capacitance of 322 F g^{-1} compared with the truncated nano-octahedrons with a specific capacitance of 244 F s^{-1} within a potential window of –0.05 to 0.95 V, and possess a good electrochemical stability, making them a promising electrode material for supercapacitors.

Acknowledgements

This work was supported by the National Natural Science Foundation of China (20925621), the Program of Shanghai Subject Chief Scientist (08XD1401500), the Shanghai Shuguang Scholars Tracking Program (08GG09).

Notes and references

1 F. Caruso, R. A. Caruso and H. Möhwald, *Science*, 1998, **282**, 1111.
2 H. B. Zeng, X. J. Xu, Y. Bando, U. K. Gautam, T. Y. Zhai, X. S. Fang, B. D. Liu and D. Golberg, *Adv. Funct. Mater.*, 2009, **19**, 3165.
3 Y. Yin and A. P. Alivisatos, *Nature*, 2005, **437**, 664.
4 A. S. Aricò, P. Bruce, B. Scrosati, J.-M. Tarascon and W. V. Schalkwijk, *Nat. Mater.*, 2005, **4**, 366.
5 C. Burda, X. B. Chen, R. Narayanan and M. A. El-Sayed, *Chem. Rev.*, 2005, **105**, 1025.
6 M. Kaempgen, C. K. Chan, J. Ma, Y. Cui and G. Gruner, *Nano Lett.*, 2009, **9**, 1872.
7 T. Y. Wei, X. H. Chen, H. C. Chien, S. Y. Lu and C. C. Hu, *Adv. Mater.*, 2009, **21**, 1.
8 *Electrochemical Supercapacitors*, ed. B. E. Conway, Kluwer-Plenum, New York, 1999.
9 L. T. Lam and R. Louey, *J. Power Sources*, 2006, **158**, 1140.
10 M. Winter and R. J. Brodd, *Chem. Rev.*, 2004, **104**, 4245.
11 R. N. Reddy and R. G. Reddy, *J. Power Sources*, 2003, **124**, 330.
12 N. Li, C. R. Martin and B. Scrosati, *Electrochem. Solid-State Lett.*, 2000, **3**, 316.
13 C. C. Hu and T. W. Tsou, *Electrochem. Commun.*, 2002, **4**, 105.
14 H. Kim and B. N. Popov, *J. Electrochem. Soc.*, 2003, **150**, D56.
15 G. M. An, P. Yu, M. J. Xiao, Z. M. Liu, Z. J. Miao, K. L. Ding and L. Q. Mao, *Nanotechnology*, 2008, **19**, 275709.
16 C.-C. Hu, Y.-T. Wu and K.-H. Chang, *Chem. Mater.*, 2008, **20**, 2890.
17 E. Katz and I. Willner, *Angew. Chem., Int. Ed.*, 2004, **43**, 6042.
18 M. C. Daniel and D. Astruc, *Chem. Rev.*, 2004, **104**, 293.
19 H. Jiang, J. Q. Hu, F. Gu, W. Shao and C. Z. Li, *Chem. Commun.*, 2009, 3618.
20 C. C. Li, K. L. Shuford, Q. H. Park, W. P. Cai, Y. Li, E. J. Lee and S. O. Cho, *Angew. Chem., Int. Ed.*, 2007, **46**, 3264.
21 X. F. Qu, G. T. Zhou, Q. Z. Yao and S. Q. Fu, *J. Phys. Chem. C*, 2010, **114**, 284.
22 T. Ghoshal, S. Biswas, P. M. G. Nambissan, G. Majumdar and S. K. De, *Cryst. Growth Des.*, 2009, **9**, 1287.
23 L. C. Zhang, Q. Zhou, Z. H. Liu, X. D. Hou, Y. B. Li and Y. Lv, *Chem. Mater.*, 2009, **21**, 5066.
24 Y. Dai, K. Wang and J. Y. Xie, *Appl. Phys. Lett.*, 2007, **90**, 104102.
25 W. Z. Ostwald, *Phys. Chem.*, 1897, **22**, 289.
26 W. Z. Ostwald, *Phys. Chem.*, 1900, **34**, 495.
27 Z. L. Wang, *J. Phys. Chem. B*, 2000, **104**, 1153.
28 M. A. Malik and Z. Khan, *Colloids Surf., B*, 2008, **64**, 42.
29 L. Rajput and K. Biradha, *Cryst. Growth Des.*, 2007, **7**, 2376.
30 H. Jiang, J. Q. Hu, C. Z. Li, F. Gu and J. Ma, *CrystEngComm*, 2010, **12**, 1726.
31 S. H. Yu and H. Colfen, *J. Mater. Chem.*, 2004, **14**, 2124.
32 Q. Zhang, S. J. Liu and S. H. Yu, *J. Mater. Chem.*, 2009, **19**, 191.
33 D. E. Zhang, X. J. Zhang, X. M. Ni, J. M. Song and H. G. Zheng, *Cryst. Growth Des.*, 2007, **7**, 2117.
34 T. Xue, C. L. Xua, D. D. Zhao, X. H. Li and H. L. Li, *J. Power Sources*, 2007, **164**, 953.
35 M. Toupin, T. Brousse and D. Belanger, *Chem. Mater.*, 2002, **14**, 3946.
36 K. A. M. Ahmed, Q. M. Zeng, K. B. Wu and K. X. Huang, *J. Solid State Chem.*, 2010, **183**, 744.
37 D. P. Dubal, D. S. Dhawale, R. R. Salnkhe, V. J. Fulari and C. D. Lokhande, *J. Alloys Compd.*, 2010, **497**, 166.
38 Z. P. Feng, G. R. Li, J. H. Zhong, Z. L. Wang, Y. N. Ou and Y. X. Tong, *Electrochem. Commun.*, 2009, **11**, 706.

